^{18}F-FDG and ^{68}Ga-FAPI PET/CT for Evaluating Periprosthetic Joint Infection and Aseptic Loosening in Rabbit Models

Yiqun Wang
Chinese PLA General Hospital
Yu Li
Chinese Academy of Sciences
Liang Han
China-Japan Union Hospital of Jilin University
Jun Wang
Chinese Academy of Sciences
Cong Zhang
Chinese PLA General Hospital
Zhiwei Guan
Chinese PLA General Hospital
Dongyun Zhang
Chinese PLA General Hospital
Yan Chang
Chinese PLA General Hospital
Yong Huan
Chinese Academy of Sciences
Jiahe Tian (www9299sss@163.com)
Chinese PLA General Hospital https://orcid.org/0000-0002-5565-3901

Research Article

Keywords: Periprosthetic joint infection, aseptic loosening, 18F-FDG, 68Ga-FAPI, rabbit model

Posted Date: January 11th, 2022

DOI: https://doi.org/10.21203/rs.3.rs-1136842/v1

Abstract

Purpose

We built a loosening model based on the original infection model of rabbit and evaluated the performance characteristics of ^{18}F-FDG and ^{68}Ga-FAPI in infection and loosening.

Methods

After surgery, the rabbits were divided into four groups, six in the control group and 10 in the loosening, *S. aureus* and *S. epidermis* groups. PET/CT and serological examination were performed every two weeks for three times. After sacrificed, micro-CT, tissue culture, pullout test and scanning electron microscope were performed.

Results

As for ^{18}F-FDG, performances of control and loosening groups were similar. SUVmax of *S. aureus* had been consistently in the high range than that of *S. epidermis*. As for ^{68}Ga-FAPI, control group had the lowest SUVmax in the second week and increased gradually. SUVmax of loosening group began exceed control group since the second week. SUVmax of *S. aureus* in the second week was the lowest among four group and raised as the number of weeks increased and equalled to SUVmax of *S. epidermis* in the sixth week. Linear regressions between SUVmax and serology showed that ^{18}F-FDG was positively correlated with CRP and IL-6 while ^{68}Ga-FAPI revealed negative and positive correlation with CRP and IL-6 in the second and sixth week. Besides, both SUVmax and MTV of ^{18}F-FDG or ^{68}Ga-FAPI were negatively correlated with BV/TV and BS/TV.

Conclusion

In this longitudinal observation, ^{68}Ga-FAPI showed greater sensitivity than ^{18}F-FDG in detecting diseases, and ^{68}Ga-FAPI had not intestinal and muscular uptake. MTV of ^{68}Ga-FAPI were larger than ^{18}F-FDG, which meant that ^{68}Ga-FAPI had the potential to define the scope of lesions more accurately. Finally, SUVmax could not differentiate loosening and infection in ^{68}Ga-FAPI, further study about diagnostic criteria was warranted.

Introduction

As aging of population and demands on the quality of life increasing, it is foreseeable that the number of joint replacements will raise persistently in the next few decades. It should be noted, however, that the

number of complications also increase, as the aseptic mechanical loosening was reported to be the most common complication and the periprosthetic joint infection (PJI) was the most devastating[1].

^{68}Ga-fibroblast activation protein (FAP) inhibitor (FAPI), as the most promising radiopharmaceutical in recent years, has been reported by more and more scholars in the field of inflammation and bone[2–5].

We have previously reported that the ^{68}Ga-FAPI exhibits totally different mechanism from ^{18}F-fludeoxyglucose (FDG) in animal model of infection[6]. In addition, a number of reports have also identified the fibrous interface in aseptic loosening[7, 8], which we think will be traced by ^{68}Ga-FAPI due to its unique mechanism.

We have already constructed a new model of infection, and in this report, we modified this animal model to mimic aseptic loosening. And the aim of this study was to explore the performance characteristics of ^{18}F-FDG and ^{68}Ga-FAPI in PJI and aseptic loosening models.

Materials And Methods

Animals

This experiment was approved by the Laboratory Animal Center of Chinese People's Liberation Army General Hospital (2020-X16-93) and thoroughly complied with the local Animal Welfare Committee. Thirty-six New Zealand White rabbits (purchased from Jinmuyang Co., Ltd, Beijing, China) were acclimated to new environment for two weeks and reared in individual cage at 24-28℃, 50-60% humidity, 12:12-h light-to-dark cycle.

Surgery

Briefly, after anesthesia (a mixed solution of midazolam, xylazine hydrochloride and sterile saline, 0.3 ml/kg), shaving, disinfecting and draping, the medial incision of left knee was chosen. Exposing capsule, self-locking screw with a diameter of 3 mm and a length of 20 mm (Biortho Medical Science and Technology Co., LTD., Jiangsu, China) were drilled and inserted into the femoral intercondylar fossa and anterior cruciate ligament footprint. It should be noted that for control and infection groups, the drill diameter was 2.5 mm and for the loosening group, the drill diameter was 3 mm to simulate the initial loosening. After suturing capsule and skin, through a 26-gauge needle, the control and loosening groups were injected 0.5 ml saline and the infection groups were with 10^5 CFU *Staphylococcus aureus* (*S. aureus*) and 10^8 CFU *Staphylococcus epidermis* (*S. epidermis* and the bacterial concentration was determined as described above[6]). Six rabbits for control group and the other groups were ten. Dressing was applied and analgesia was performed for three days after surgery. For control and loosening group, penicillin was injected for three days postoperatively, while no prophylactic antibiotics for infection groups.

PET/CT

PET/CT (uMI510, United Imaging Healthcare, Shanghai, China) was performed every two weeks and ^{18}F-FDG and ^{68}Ga-FAPI were selected randomly. ^{18}F-FDG was synthesized according to method described by Hamacher et al.[9] with modification through a computer-controlled apparatus. ^{68}Ga-FAPI (TanzhenBio Co., Ltd, Nanchang, China) was synthesized in-house as previously reported[6]. After sedation (a mixture solution xylazine hydrochloride, chlorpromazine and sterile saline, 0.6ml per rabbit), each rabbit was injected about 37 MBq (1 mCi) and scanned one hour later. PET acquisition time was 5 min for both ^{18}F-FDG and ^{68}Ga-FAPI with one bed position. The attenuation was corrected using CT data and the image was reconstructed using the standard ordered-subset expectation maximization algorithm. The dead time, decay, photon attenuation and the other effects were corrected for PET data.

Two independent, junior nuclear medicine physicians blinded to the radiopharmaceuticals, the weeks of examination and the grouping were trained by a senior nuclear medicine physician to draw 3D view of interest (VOI). It was considered feasible that the results of maximum standardized uptake value (SUVmax) were consistent. If the difference between the calculation of mean SUV (SUVmean) and metabolic target volume (MTV) were less than 20%, the data were considered valid and the final value were represented as the average of the two-corresponding data[6].

Serological examination

Blood samples were drawn from the central ear arteries and sandwich ELISA (RayBiotech Life, Inc.) was used to detect C-reactive protein (CRP), interleukin-6 (IL-6) and FAP every two weeks after operation according to the instruction.

Micro-CT

Rabbits were euthanized by injecting an overdose of sodium pentobarbital intravenously. The part from the lower 1/2 of femur to the upper 1/2 of tibia was completely amputated through the aseptic technique. After wrapping by sterile preservative film, micro-CT (Quantum GX2, PerkinElmer, Waltham, Massachusetts, USA) was performed with 90 kV, 88 uA, FOV of 72 for four minutes. The bone surface (BS)/bone volume (BV), BS/tissue volume (TV) and BV/TV were calculated for the targeted VOI.

Tissue culture and pathology

After Micro-CT, the soft tissue around the knee was dissected, partly for tissue culture, no bacteria grow for 72 hours was defined as negative. And partly for pathological examination which include two parts, H&E and immunohistochemistry (IHC), according previously reported[10].

Pullout test and scanning electron microscope (SEM)

Finally, the tibia containing screw went pullout test and screw from femur went SEM. As for pullout test (Fig. 1a-d), the soft tissue around the tibia was removed as much as possible and the distal end of the screw was exposed, then fastening this bone block with denture acrylic. When the denture acrylic solidified, the shape of the bone block was cutting to make the screw perpendicular to the ground when the bone block was placed on the objective table. The machine was started when the detector was

adjusted to about 1 mm above the distal end of the screw with 5 Hz/s and the maximum force value was recorded. As for SEM, screw removed from femur was fixed in 2.5% glutaric dialdehyde for 24 hours and rinsed with distilled water for three times and then dehydrated in freeze drier. After screw was mounted on an aluminum block stub and sputter-coated with gold-palladium, Micro-CT (Quantum GX2, PerkinElmer, Waltham, Massachusetts, USA) was performed.

Statistical analysis

Data were expressed as mean ± standard deviation (SD). Paired t test was used for intra-group comparison and analysis of variance (ANOVA) was used for inter-group comparison. Correlations between PET-derived metrics and other tests were analyzed by Pearson's rank correlation. All tests were 2-tailed and p-value < 0.05 was considered as statistically significant. GraphPad Prism 8.0.2 (GraphPad Software, San Diego, CA, USA) was used to perform statistical analyses.

Results

Tissue cultures of control group were all negative. One rabbit from loosening group developed femoral fracture during surgery (Supplementary Figure 1) and one was tissue culture positive. One rabbit from *S. aureus* died after two weeks and two died after four weeks and two rabbits from *S. epidermis* did not develop infection. All mentioned rabbits were excluded from further analysis.

Model Validation

The pullout strength of control was 273.43±12.96 N. In loosening and *S. epidermis*, the values were 222.24±19.88 N and 249.31±26.98 N. The pullout strength of *S. aureus* was 176.91±52.09 N (Fig. 1e-i), which could be attributed to the cortical bone destruction by *S. aureus*.

Screws from femur were subjected to SEM (Fig. 2). In control, the thread of screw was clearly visible. In loosening, ruptured fibrous membrane could be observed. In *S. aureus*, a large number of bacteria and an extensive biofilm were formed. In *S. epidermis*, small amounts of bacteria and scarce biofilm could be detected. All of these results demonstrated that the feasibility of this animal model.

PET/CT examination

In control group, there was no significant uptake of ^{18}F-FDG in the second week, nor in the fourth or sixth week. As for ^{68}Ga-FAPI, the second week had the lowest SUVmax which was gradually increased in the following tests (Fig. 3a). Since arthritis and osteophyte could express FAP and this surgery could also cause damage in the joint, it was assumed that the degeneration was happened in this model.

In loosening group (Fig. 3b), the manifestations of ^{18}F-FDG were similar with those of the control group. As for ^{68}Ga-FAPI, the mean value of SUVmax was larger than those of the control group since the second week.

In *S. aureus* group (Fig. 3c), SUVmax of ^{18}F-FDG was persistently in a relatively high range, while the SUVmax of ^{68}Ga-FAPI showed a completely different performance. In the second week, SUVmax of ^{68}Ga-FAPI was the lowest among four group (P<0.05). As the number of weeks increased, so did the value of SUVmax and in the sixth week, the mean value of ^{68}Ga-FAPI was highest among four group (no significant difference). No basic research had been focused on this phenomenon and our previous report had made assumptions about it. Furthermore, MTV of ^{18}F-FDG and ^{68}Ga-FAPI were all larger than other groups in corresponding week.

In *S. epidermis* group (Fig. 3d), SUVmax of both ^{18}F-FDG and ^{68}Ga-FAPI in the second week were not statistically significant from those of control groups and then were gradually increased, and in the sixth week, those of *S. epidermis* were significantly different from those of control (P<0.05). Since the leucocyte chemotaxis of *S. epidermis* was far weaker than that of *S. aureus*, so it was foreseeable that ^{18}F-FDG could not initially show the disease well. As for ^{68}Ga-FAPI, although there was no statistical difference between *S. epidermis* and loosening in the second week, the average value of SUVmax of *S. epidermis* was higher than that of loosening (4.0±0.8 VS 3.3±0.6), in addition, performance characteristics of *S. epidermis* were different from those of *S. aureus* and it was speculated that the low-virulent bacteria could increase the secretion of FAP in a certain degree.

As for SUVmean, no clear conclusions could be drawn independently of SUVmax. Furthermore, in clinical cases, it was easy to draw a VOI around solid tumors, but was hard to draw around hip prosthesis, which also limited it use, so did the SUVpeak and total lesion glycolysis or total lesion FAPI.

As far as MTV concerned, it also had the limitation mentioned above, but one thing should be noted that almost all MTV of ^{68}Ga-FAPI were larger than those of ^{18}F-FDG, which was in accord with our previous report and this property might allow ^{68}Ga-FAPI to be more sensitive and to view a wider range of lesion.

Pathological analysis

Pathology was performed to validate the consistency of PET/CT in the sixth week (Fig. 4). H&E showed that an abundant of leukocytes were expressed in groups of *S. aureus* and *S. epidermis* and in loosening group, plentiful activated fibroblasts were detected. IHC included CD45 and FAP. Striking CD45 were expressed in *S. aureus* and *S. epidermis*. As for FAP, loosening, *S. aureus* and *S. epidermis* all had intense expression and control also had moderate expression. Above-mentioned results conformed with the results of PET/CT.

Serological examination

As for serological results (Fig. 5), the highest levels of CRP and IL-6 were found in *S. aureus* in all weeks, followed by *S. epidermis*. The CRP levels between control and loosening groups were not significant, however, the IL-6 levels of loosening were statistically significant from those of control in the fourth and sixth week. As for FAP, there were no clear conclusions could be drawn in intra- or inter-group comparison,

which was unexpected and yet somehow reasonable, since several articles had reported that some diseases had FAP expression, but serum FAP remains unchanged.

Next, linear regressions between SUVmax and serological results were performed. As for ^{18}F-FDG, SUVmax was positively correlated with CRP and IL-6, however, 68Ga-FAPI showed a completely different performance. In all weeks, there was no significant correlation between SUVmax of ^{68}Ga-FAPI and CRP and IL-6, while SUVmax showed negative and positive correlation with CRP and IL-6 in the second and sixth week respectively. This phenomenon indicated that FAP was less expressed at the lesion site in the early stage of systemic inflammation and more expressed in the late stage, especially infection. Whether this property of ^{68}Ga-FAPI led to a weaker role in acute infection or to a new therapeutic target for chronic infection deserved further study. As for serum FAP, there was no significant correlation with SUVmax, either ^{18}F-FDG or ^{68}Ga-FAPI (data not shown).

Micro-CT

Micro-CT was performed to observe the change of the bone (Fig. 6). It was obvious that the morphology of *S. aureus* was severely corroded to the naked eyes, which was unsurprising that *S. aureus* was far more erosive than *S. epidermis*.

BV/TV and BS/TV of *S. aureus* were significantly different from other groups ($P<0.05$) and BV/TV of *S. epidermis* was significantly different from control and loosening ($P<0.05$) and BS/TV was statistically significant from loosening ($P<0.05$). The expression of FAP was thought to be associated with bone erosion, so the linear regressions between SUVmax, SUVmean and MTV and BV/TV and BS/TV were performed. Although both SUVmax and MTV of ^{18}F-FDG or ^{68}Ga-FAPI were negatively correlated with BV/TV and BS/TV, yet the MTV of ^{68}Ga-FAPI was more sensitive than other indicators.

Discussion

The aim of this study was to build a loosening model based on the previous model and evaluate the performance characteristics of ^{18}F-FDG and ^{68}Ga-FAPI in rabbit models of *S. aureus*, *S. epidermis*, control and loosening.

Unexpected, but reasonable, *S. aureus* and *S. epidermis* showed different uptake patterns in longitudinal observation. In second week of ^{68}Ga-FAPI, the SUVmax and SUVmean of *S. aureus* were far less than those of *S. epidermis*. In the next two tests, the values of *S. aureus* rose significantly and were equal to those of the *S. epidermis*. As for loosening group, a narrow range of high uptake was observed since the fourth week, which was believed to be caused by the friction between the loose screw and the articular cavity activating fibroblast. Although the SUVmax of the sixth week of loosening, *S. aureus* and *S. epidermis* were nearly same, their changes were markedly different over the course of the three tests. Meanwhile, MTV of loosening was larger than that of control group and uptake was visible along the loosening screw, which all demonstrated that ^{68}Ga-FAPI has certain application value in prosthesis

loosening. As for ^{18}F-FDG, although SUVmax and SUVmean of *S. aureus* were significantly larger than those of *S. epidermis* in all three tests, discrimination of control and loosening group was blurry. Besides, almost all MTV of ^{68}Ga-FAPI were larger than ^{18}F-FDG. To sum up, mechanics of bacterial imaging of ^{68}Ga-FAPI was different from that of ^{18}F-FDG and in loosening imaging, ^{68}Ga-FAPI showed higher sensitivity. The present study demonstrated the feasibility of ^{68}Ga-FAPI in assessing symptomatic joint replacement.

Cause of loosening contains two major aspects, namely abrasion particles and initial instability[7]. At the present study, we constructed a new loosening model based on second mode. There had already existed several loosening models, including air pouching model of murine, and debris-induced loosening model of murine and rabbit[11–16]. The original aim of debris-induced loosening model was to simulate the situation that bone cement, metal and etc. stimulate macrophages to produce absorptive stimulators leading to osteolysis. Clinically, we could also see the widening of the medullary cavity in patients with loosening and combined with the above, this was also an instability. This property was similar to the initial instability, which was why we build this loosening model. Besides, the head of the screw received continuous force in the articular cavity, which was closer to the real clinical situation. Meanwhile, SEM was used to observe the surface of screw and rupture fibrous membrane was found in loosening group, which further proved the feasibility of this model.

For the test of mechanical stability, some scholars used the same force to record the different displacements of the screws[17], while others recorded the maximum force at which the screw detached from the bone[15, 16], that was the pullout strength. The latter method was used in this experiment. *S. aureus* was the lowest of all groups and the micro-CT confirmed it. The pullout strength of control was higher than that of She et al., this may be due to the different examination sites and implants. The pullout strength of loosening was lower than their report, which may mean that this model had the potential to be faster and more significant.

Although the application of ^{68}Ga-FAPI in PJI has not been reported yet, the advantages of ^{68}Ga-FAPI over ^{18}F-FDG could be seen from this experiment and other reports[18–22]. Firstly, ^{68}Ga-FAPI was more sensitive to disease detection. It can detect degeneration and loosening of joint, let alone the infections. Speaking of this, how to distinguish between infection and loosening. Although the SUVmax of these groups were similar, their variations were different, combined with MTV, which suggests that loosening and infection may have different uptake patterns in the clinic and we did find that different uptake patterns in loosening and infection in clinical cases (Supplementary Figure 2). Besides, with the development of PET/CT radiomics[23, 24], whether this method could be used to diagnose the kinds of bacteria that are infected is also a very interesting and attractive field. Secondly, ^{68}Ga-FAPI did not have nonspecific uptake of muscle and intestinal than ^{68}Ga-FAPI, which could increase the specificity of ^{68}Ga-FAPI. Thirdly, ^{68}Ga-FAPI does not require fasting and shows a broader range of lesions with clearer boundaries and the waiting time for examination may be shorter.

There were several limitations in this study. Due to the limited number, pathology of the second and the fourth weeks were not performed. Then, many phenomena found in this experiment need to be studied in basic experiments. Finally, this study was only on animals, clinical studies were urgently needed to verify the feasibility of ^{68}Ga-FAPI.

Conclusion

In this study, SEM and pullout test were used to validate the feasibility of a new loosening model. And in the longitudinal observation of control, loosening, *S. aureus* and *S. epidermis*, ^{68}Ga-FAPI showed greater sensitivity and specificity than ^{18}F-FDG in detecting diseases. Besides, almost all MTV of ^{68}Ga-FAPI were larger than those of ^{18}F-FDG, which meant that ^{68}Ga-FAPI had the potential to define the scope of lesions more accurately. Taken together, these results suggest that ^{68}Ga-FAPI has great potential in the diagnosis of PJI and has distinct advantages over ^{18}F-FDG. However, the diagnostic efficacy of SUVmax was not satisfied in ^{68}Ga-FAPI and further study about diagnostic criterion and basic research about the mechanism of FAP in infection and the expression site of FAP in infection is warranted.

Declarations

Funding

This work is supported by the National Natural Science Foundation of China (Grant number 11972037).

Conflict of interest

No conflicts of interest exist with regard to this submission.

Authors' contributions

Y.Q.W., Y.L and L.H wrote the original draft, J.W. and Q.X.L. ran the data curation and formal analysis, and Z.W.G. and D.Y.Z. used the softwares, Y.H. and Y.C. was supervision and designed the project, J.H.T. was supervision and reviewed and edited the draft.

Ethics approval

This research was approved by the Laboratory Animal Center of Chinese People's Liberation Army General Hospital (2020-X16-93) and all related experiments were strictly complied with the local Animal Welfare Committee.

References

1. Hoskins W, Rainbird S, Peng Y, Lorimer M, Graves SE, Bingham R. Incidence, Risk Factors, and Outcome of Ceramic-On-Ceramic Bearing Breakage in Total Hip Arthroplasty. The Journal of

arthroplasty. 2021;36(8):2992–7. doi:10.1016/j.arth.2021.03.021.

2. Qin C, Song Y, Liu X, Gai Y, Liu Q, Ruan W et al. Increased uptake of (68)Ga-DOTA-FAPI-04 in bones and joints: metastases and beyond. European journal of nuclear medicine and molecular imaging. 2021. doi:10.1007/s00259-021-05472-3.
3. Schmidkonz C, Rauber S, Atzinger A, Agarwal R, Götz TI, Soare A et al. Disentangling inflammatory from fibrotic disease activity by fibroblast activation protein imaging. Annals of the rheumatic diseases. 2020;79(11):1485–91. doi:10.1136/annrheumdis-2020-217408.
4. Hao B, Wu X, Pang Y, Sun L, Wu H, Huang W et al. [(18)F]FDG and ([68)Ga]Ga-DOTA-FAPI-04 PET/CT in the evaluation of tuberculous lesions. European journal of nuclear medicine and molecular imaging. 2021;48(2):651–2. doi:10.1007/s00259-020-04941-5.
5. Luo Y, Pan Q, Zhang W, Li F. Intense FAPI Uptake in Inflammation May Mask the Tumor Activity of Pancreatic Cancer in 68Ga-FAPI PET/CT. Clinical nuclear medicine. 2020;45(4):310–1. doi:10.1097/rlu.0000000000002914.
6. Wang Y, Liu H, Yao S, Guan Z, Li Q, Qi E et al. Using 18F-flurodeoxyglucose and 68Ga-fibroblast activation protein inhibitor PET/CT to evaluate a new periprosthetic joint infection model of rabbit due to Staphylococcus aureus. 9000. doi:10.1097/mnm.0000000000001495.
7. Morawietz L, Classen RA, Schröder JH, Dynybil C, Perka C, Skwara A et al. Proposal for a histopathological consensus classification of the periprosthetic interface membrane. Journal of clinical pathology. 2006;59(6):591–7. doi:10.1136/jcp.2005.027458.
8. Weissman BN. Imaging of total hip replacement. Radiology. 1997;202(3):611–23. doi:10.1148/radiology.202.3.9051004.
9. Hamacher K, Coenen HH, Stöcklin G. Efficient stereospecific synthesis of no-carrier-added 2-[18F]-fluoro-2-deoxy-D-glucose using aminopolyether supported nucleophilic substitution. Journal of nuclear medicine: official publication, Society of Nuclear Medicine. 1986;27(2):235–8.
10. Han L, Liu D, Li Z, Tian N, Han Z, Wang G et al. HOXB1 Is a Tumor Suppressor Gene Regulated by miR-3175 in Glioma. PloS one. 2015;10(11):e0142387. doi:10.1371/journal.pone.0142387.
11. Wooley PH, Morren R, Andary J, Sud S, Yang SY, Mayton L et al. Inflammatory responses to orthopaedic biomaterials in the murine air pouch. Biomaterials. 2002;23(2):517–26. doi:10.1016/s0142-9612(01)00134-x.
12. Warme BA, Epstein NJ, Trindade MC, Miyanishi K, Ma T, Saket RR et al. Proinflammatory mediator expression in a novel murine model of titanium-particle-induced intramedullary inflammation. Journal of biomedical materials research Part B, Applied biomaterials. 2004;71(2):360–6. doi:10.1002/jbm.b.30120.
13. Yang SY, Yu H, Gong W, Wu B, Mayton L, Costello R et al. Murine model of prosthesis failure for the long-term study of aseptic loosening. Journal of orthopaedic research: official publication of the Orthopaedic Research Society. 2007;25(5):603–11. doi:10.1002/jor.20342.
14. Ren W, Zhang R, Hawkins M, Shi T, Markel DC. Efficacy of periprosthetic erythromycin delivery for wear debris-induced inflammation and osteolysis. Inflammation research: official journal of the

European Histamine Research Society [et al]. 2010;59(12):1091–7. doi:10.1007/s00011-010-0229-x.

15. Zhu FB, Cai XZ, Yan SG, Zhu HX, Li R. The effects of local and systemic alendronate delivery on wear debris-induced osteolysis in vivo. Journal of orthopaedic research: official publication of the Orthopaedic Research Society. 2010;28(7):893–9. doi:10.1002/jor.21062.
16. She C, Shi GL, Xu W, Zhou XZ, Li J, Tian Y et al. Effect of low-dose X-ray irradiation and Ti particles on the osseointegration of prosthetic. Journal of orthopaedic research: official publication of the Orthopaedic Research Society. 2016;34(10):1688–96. doi:10.1002/jor.23179.
17. Schroeder K, Simank HG, Lorenz H, Swoboda S, Geiss HK, Helbig L. Implant stability in the treatment of MRSA bone implant infections with linezolid versus vancomycin in a rabbit model. Journal of orthopaedic research: official publication of the Orthopaedic Research Society. 2012;30(2):190–5. doi:10.1002/jor.21516.
18. Pang Y, Zhao L, Luo Z, Hao B, Wu H, Lin Q et al. Comparison of (68)Ga-FAPI and (18)F-FDG Uptake in Gastric, Duodenal, and Colorectal Cancers. Radiology. 2021;298(2):393–402. doi:10.1148/radiol.2020203275.
19. Chen H, Pang Y, Wu J, Zhao L, Hao B, Wu J et al. Comparison of [(68)Ga]Ga-DOTA-FAPI-04 and [(18)F] FDG PET/CT for the diagnosis of primary and metastatic lesions in patients with various types of cancer. European journal of nuclear medicine and molecular imaging. 2020;47(8):1820–32. doi:10.1007/s00259-020-04769-z.
20. Luo Y, Pan Q, Yang H, Peng L, Zhang W, Li F. Fibroblast Activation Protein-Targeted PET/CT with (68)Ga-FAPI for Imaging IgG4-Related Disease: Comparison to (18)F-FDG PET/CT. Journal of nuclear medicine: official publication, Society of Nuclear Medicine. 2021;62(2):266–71. doi:10.2967/jnumed.120.244723.
21. Lan L, Liu H, Wang Y, Deng J, Peng D, Feng Y et al. The potential utility of [(68) Ga]Ga-DOTA-FAPI-04 as a novel broad-spectrum oncological and non-oncological imaging agent-comparison with [(18)F]FDG. European journal of nuclear medicine and molecular imaging. 2021. doi:10.1007/s00259-021-05522-w.
22. Giesel FL, Kratochwil C, Schlittenhardt J, Dendl K, Eiber M, Staudinger F et al. Head-to-head intra-individual comparison of biodistribution and tumor uptake of (68)Ga-FAPI and (18)F-FDG PET/CT in cancer patients. European journal of nuclear medicine and molecular imaging. 2021. doi:10.1007/s00259-021-05307-1.
23. Wu Q, Wang S, Li L, Wu Q, Qian W, Hu Y et al. Radiomics Analysis of Computed Tomography helps predict poor prognostic outcome in COVID-19. Theranostics. 2020;10(16):7231–44. doi:10.7150/thno.46428.
24. Mu W, Jiang L, Zhang J, Shi Y, Gray JE, Tunali I et al. Non-invasive decision support for NSCLC treatment using PET/CT radiomics. Nature communications. 2020;11(1):5228. doi:10.1038/s41467-020-19116-x.

Figures

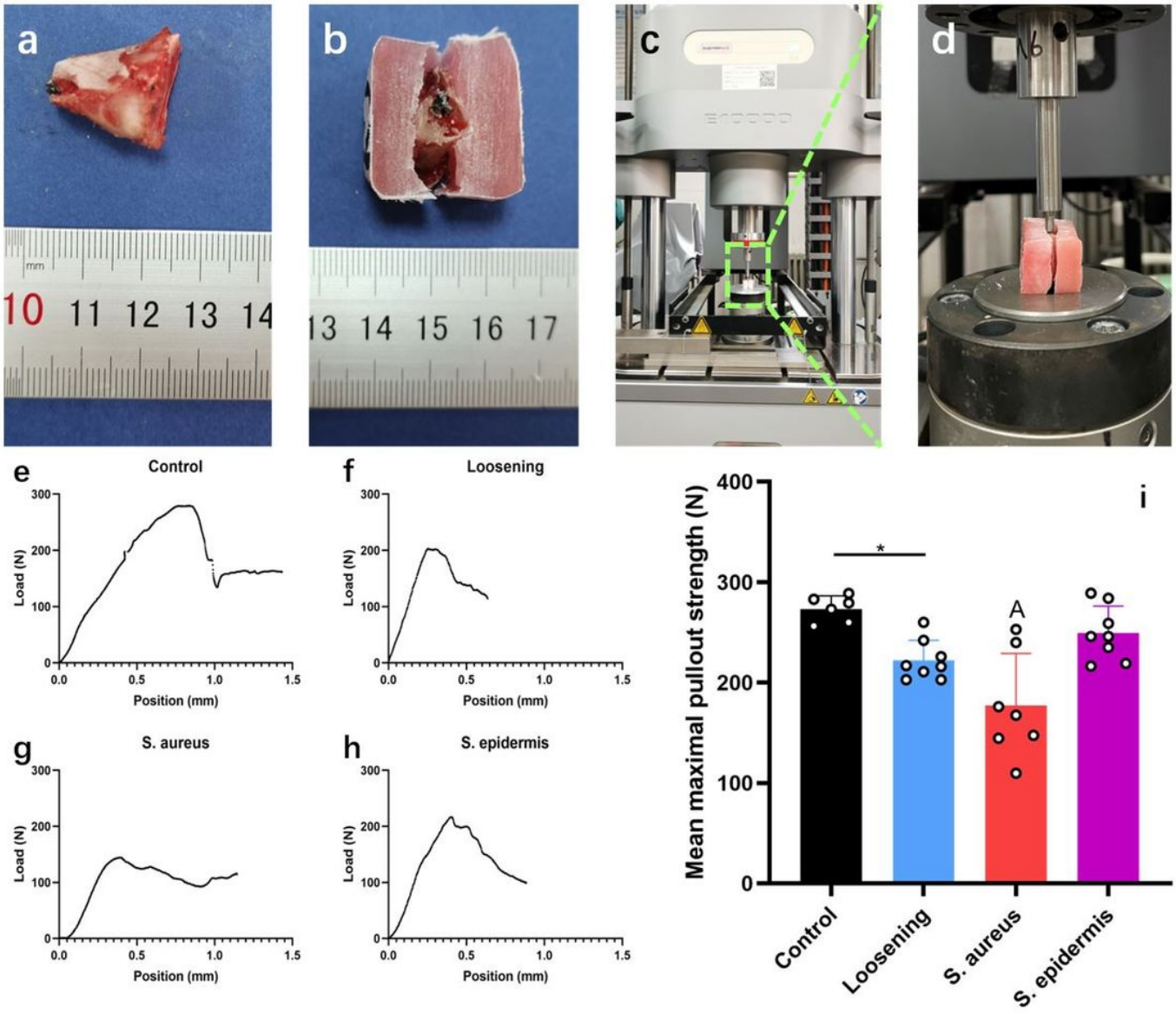

Figure 1

Pullout test. a, soft tissue was removed from tibia. b, bone block was fastened by denture acrylic. c, distant view of machine. d, close-up view of objective table. e, representative image of pullout strength of control group. f, representative image of pullout strength of loosening group. g, representative image of pullout strength of S. aureus group. h, representative image of pullout strength of S. epidermis group. i, mean maximal pullout strength of four groups. *, $P < 0.05$; A, significantly different from other groups ($P < 0.05$).

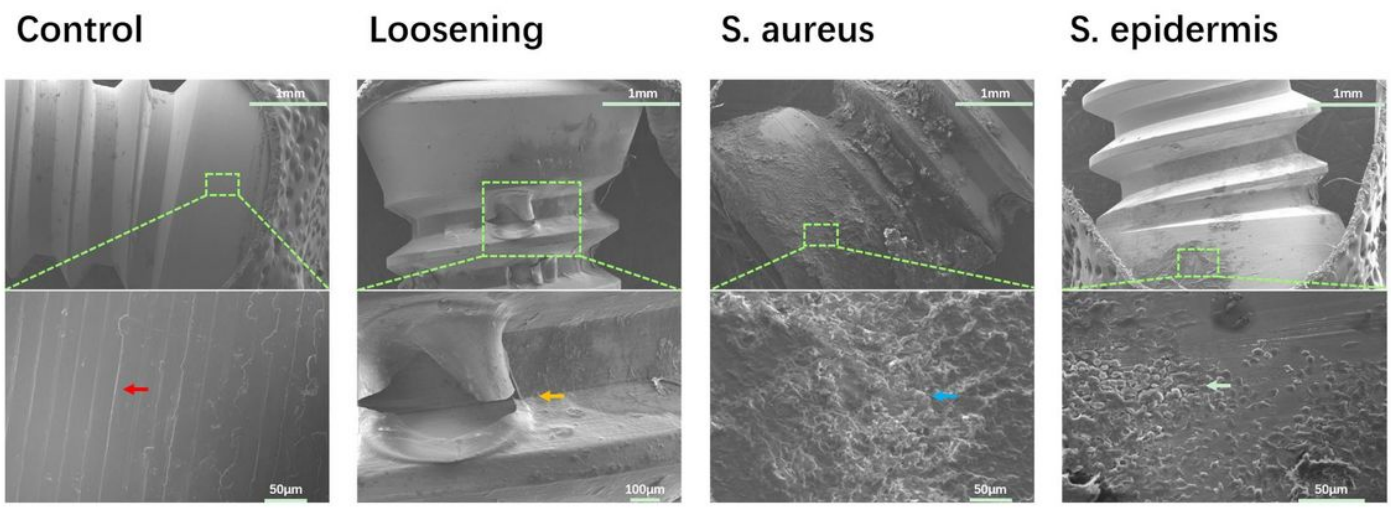

Figure 2

Scanning electron microscope images of proximal end of screw from femur. Micrographs on the upper panels show the sections of entire screws. Micrographs on the lower panels represent magnifications of the area framed in the fluorescent green box. Images are representative of five replicates with similar results. Red arrow, thread of screw. Brown arrow, ruptured fibrous membrane. Blue arrow, biofilm-like extracellular matrix. White arrow, sparse microflora.

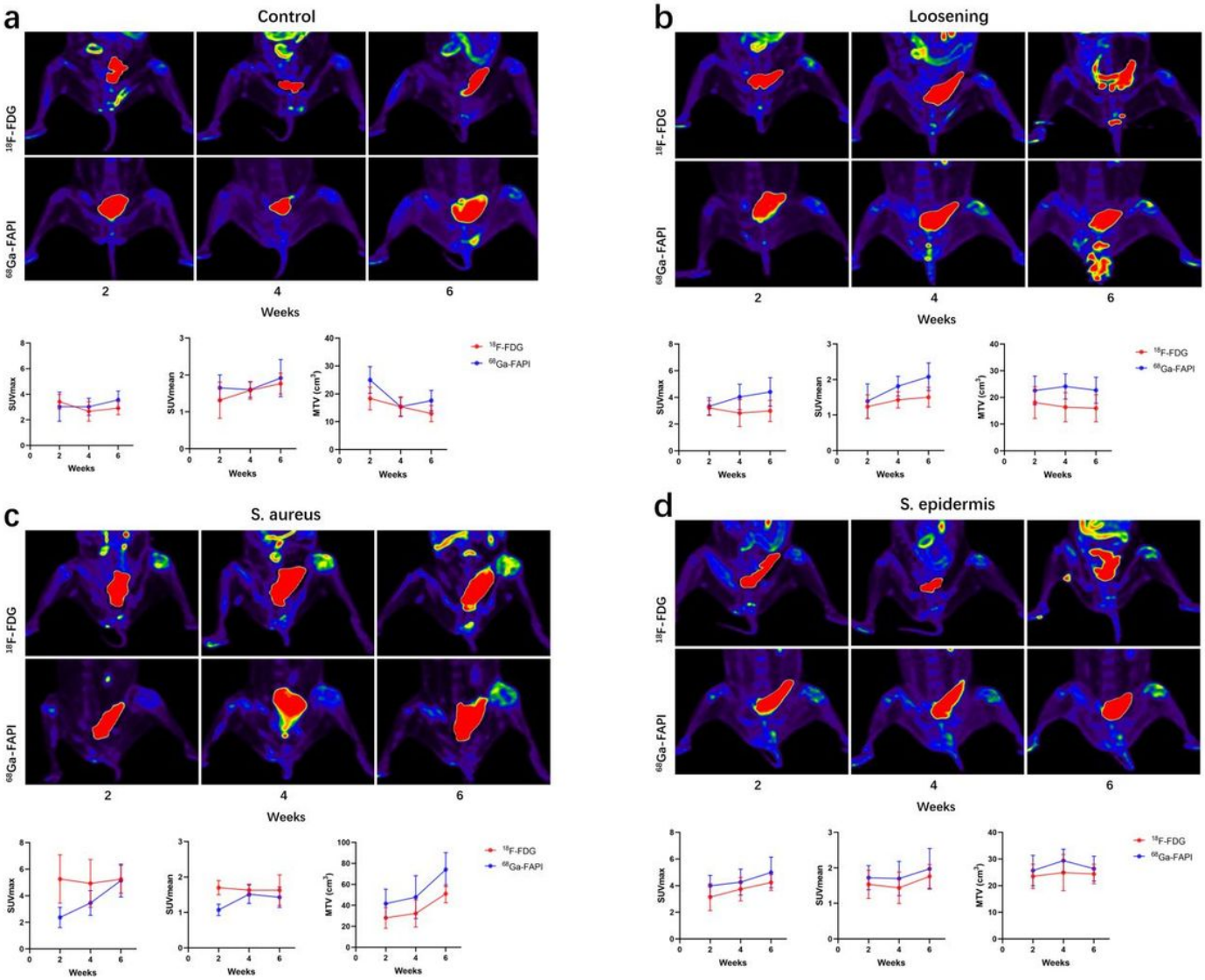

Figure 3

Representative images and results of SUVmax, SUVmean and MTV of each group.

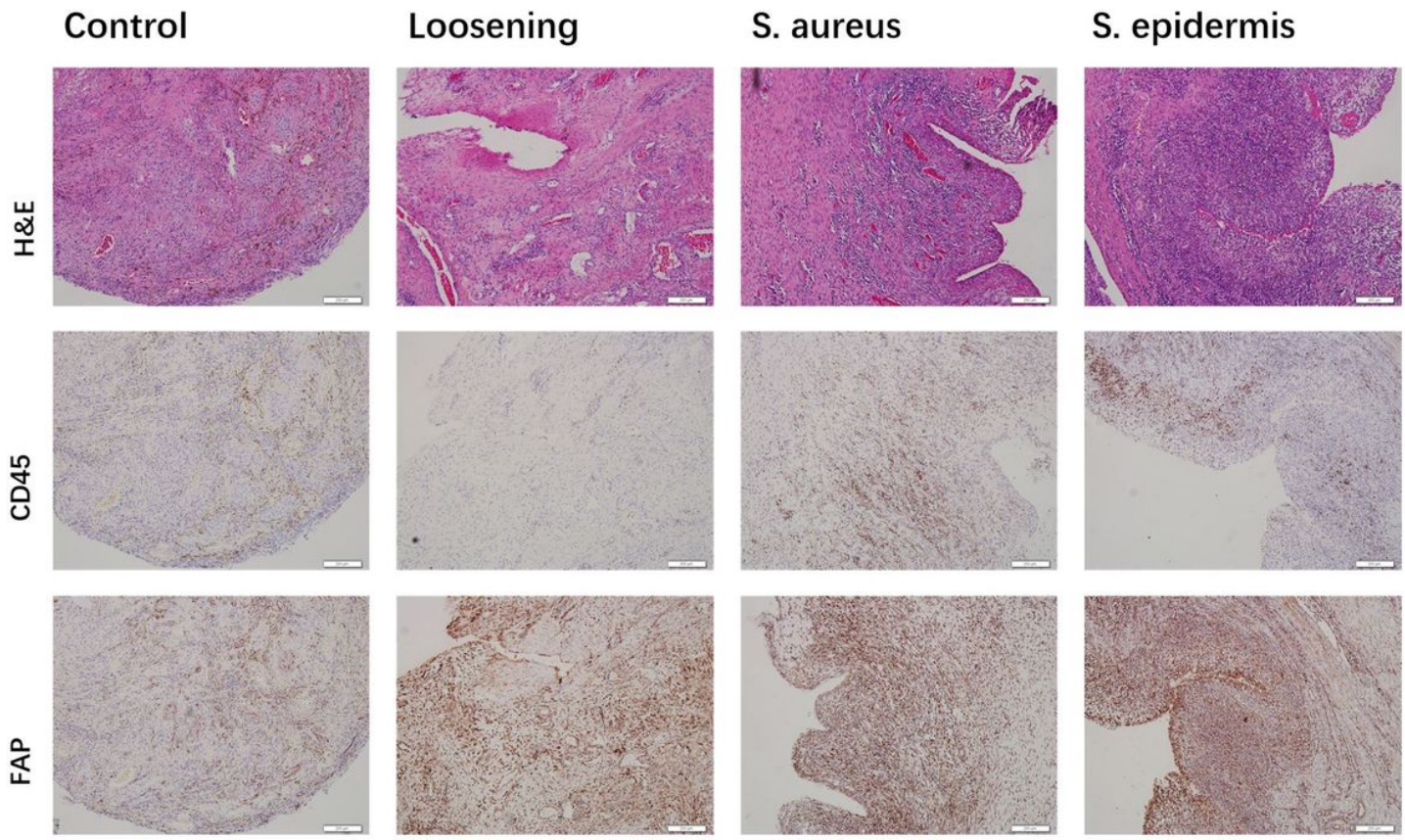

Figure 4

Analysis of models by pathology in parallel PET/CT scan in the sixth week. First row: representative H&E stainings showing abundant leukocyte in S. aureus and S. epidermis and activated fibroblast in loosening; second and third row: immunohistochemistry for CD45 and FAP. Images are representative of five biological replicates.

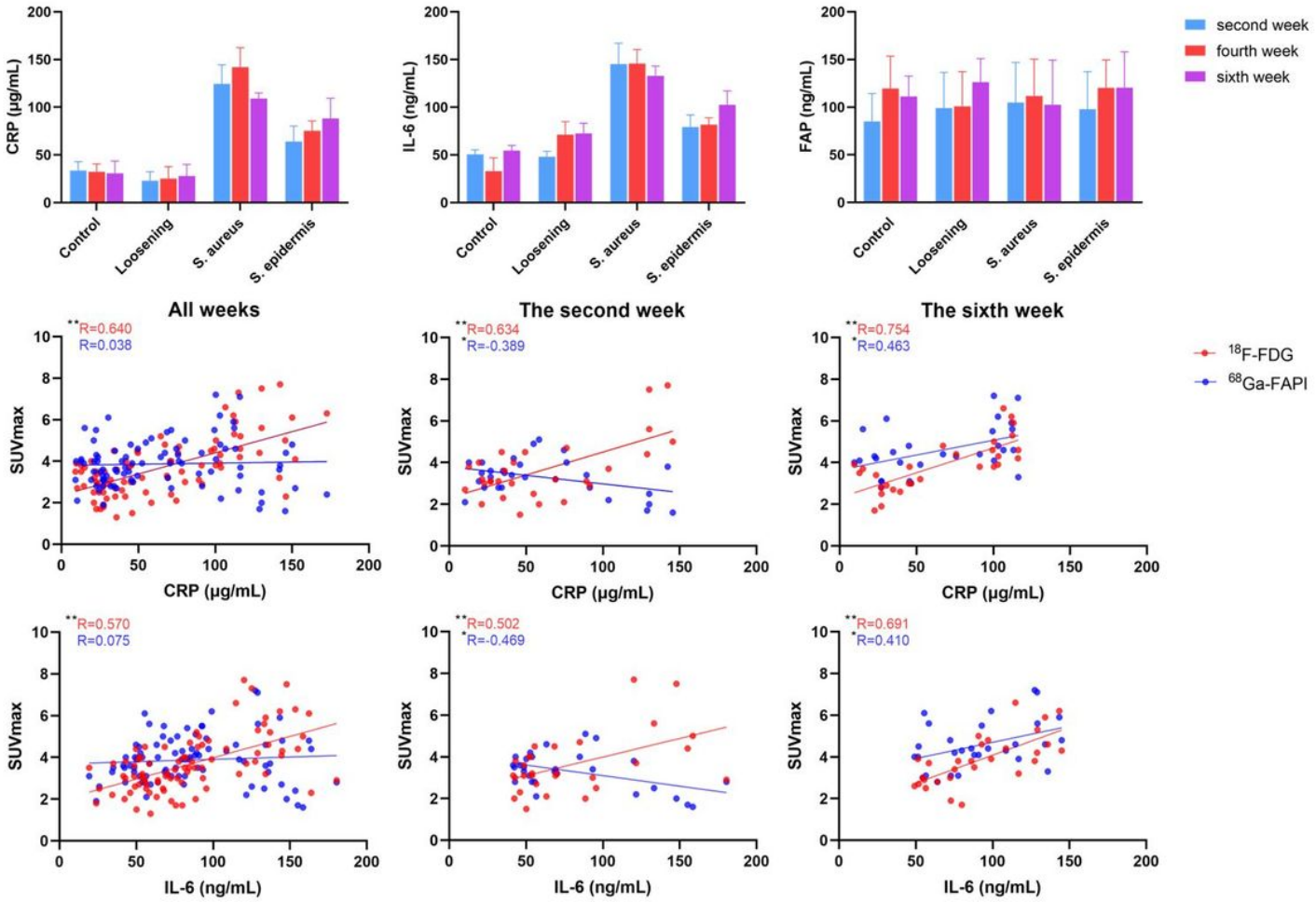

Figure 5

Physical and Serological examination. a, results of CRP, IL-6 and FAP. b, correlations between SUVmax of ^{18}F-FDG and ^{68}Ga-FAPI and serological results of CRP, IL-6 and FAP in the second, sixth and all weeks. c, results of changes of weight, knee width and temperature. *, $P < 0.05$; **, $P < 0.01$.

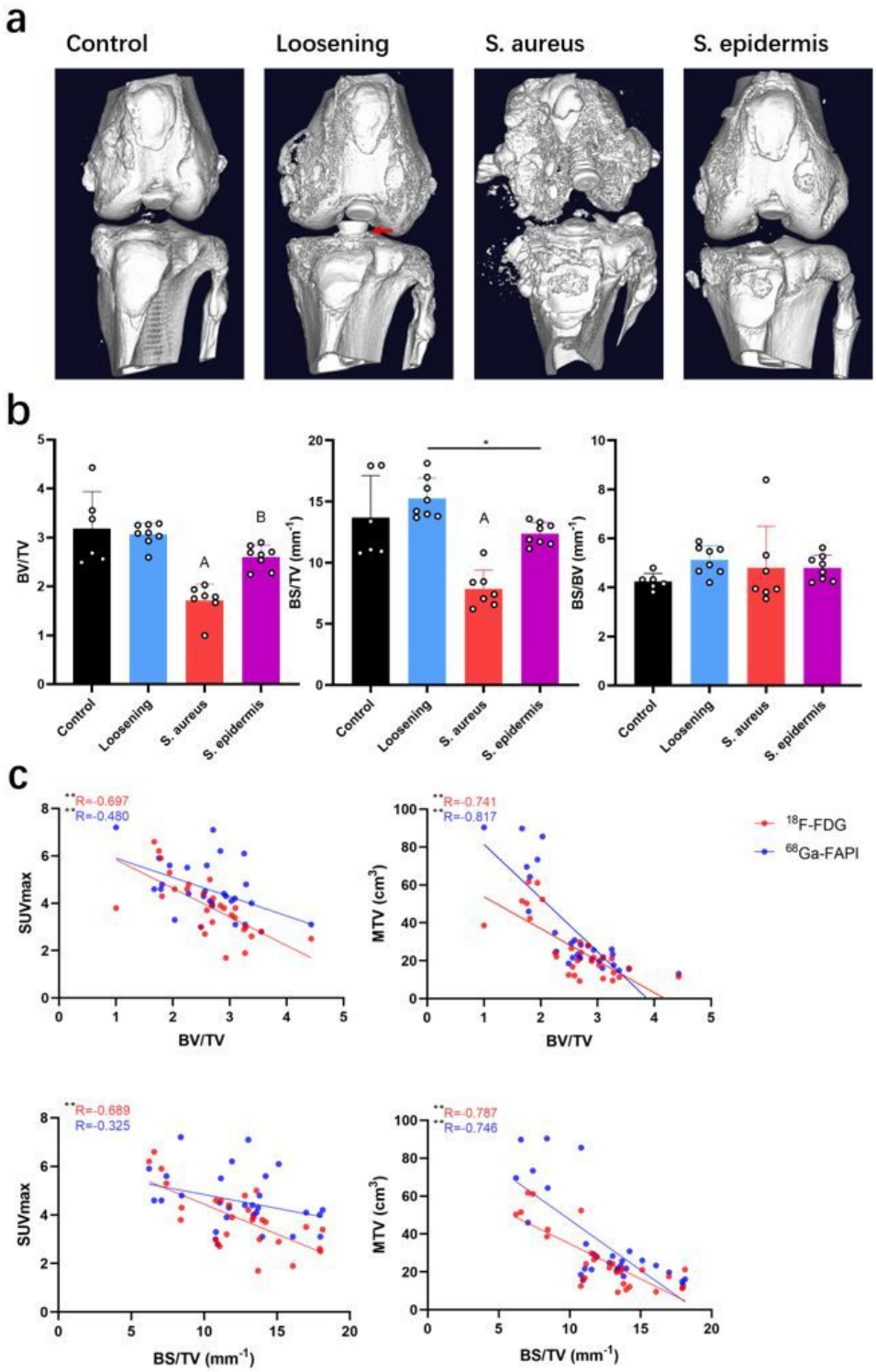

Figure 6

Micro-CT. a, representative images. b, results of BV/TV, BS/TV and BS/BV. *, P < 0.05; A, significantly different from other groups (P < 0.05); B, significantly different from groups of control and loosening. Red arrow, retreat of screw.

Supplementary Files

This is a list of supplementary files associated with this preprint. Click to download.

- Supplementaryfigure.docx